CrossMark

Microstructural and Mechanical Properties of Hot Roll Bonded Titanium Alloy/Low Carbon Steel Plate

Chao Yu, Zi-chen Qi, Hui Yu, Cheng Xu, and Hong Xiao

In this paper, a titanium alloy and low carbon steel were bonded via hot rolling in a vacuum, and the effect of roll bonding temperature and reduction ratio on the microstructural and mechanical properties of the plate was studied. When the bonding temperature was between 850 and 1050 °C, the shear strength of the interface increased with an increasing reduction ratio from 18 to 70%. At a bonding temperature of 950 °C and at a rolling reduction ratio of 70%, the best bonding strength was obtained, and a shear fracture occurred on the low carbon steel matrix. At 1050 °C, brittle compounds, i.e., TiC, FeTi, and Fe$_2$Ti, formed at the interface, which decreased the bonding strength. The large reduction ratio can break up compounds at the interface and extrude fresh metal for bonding, thereby increasing the bonding strength.

1. Introduction

Titanium clad steel plates not only have the corrosion resistance of titanium but also have the good mechanical properties of steel; moreover, they save precious titanium metals (Ref 1-3). Due to these characteristics, titanium clad steel plates are widely used in the petrochemical, shipbuilding, and marine industries, among others (Ref 4-7). Currently, several methods are used to manufacture titanium clad steel plates, such as diffusion bonding, explosive welding, explosive roll bonding, and roll bonding (Ref 8-11).

Momono et al. (Ref 12) studied the effect of carbon content on the diffusion bonding of steel to titanium. At a bonding temperature above 900 °C, the intermetallic compounds FeTi and Fe$_2$Ti formed at the bond interface in the bonding of titanium to steel with 0.01% C, and TiC, FeTi, and Fe$_2$Ti formed when using steel with 0.19% C. The bond strength decreased with the growth of the compound layer. In a study of a hot roll bonded titanium/low carbon steel plate, Yu et al. (Ref 13) found that TiC formed at the titanium/low carbon steel interface at a bonding temperature of 850 °C and with a reduction ratio of 25%. The formation of TiC, FeTi, and Fe$_2$Ti was effectively inhibited upon using a pure iron interlayer at 850 °C. However, when the temperature was as much as 950 °C, TiC, FeTi, and Fe$_2$Ti were generated at the bonding interface of titanium and pure iron, significantly decreasing the bonding strength. Similarly, Jiang et al. (Ref 14) found that at a heat treatment temperature of 850 °C or below, TiC formed near the titanium side of the titanium/steel explosive-rolling

clad plate interface. At 950 °C, FeTi and Fe$_2$Ti were generated near the steel side of the interface with a small amount of TiC generated during the diffusion reaction, decreasing the bonding strength.

Compared with diffusion bonding and explosive welding, the roll bonding method can produce large-sized and thin titanium clad steel plates with a high production efficiency (Ref 15, 16). Using roll bonding is a trend in composite plate production. Because brittle compounds, such as TiC, FeTi, and Fe$_2$Ti, reduce the titanium clad steel plate bonding strength, a method using an intermediate layer material is commonly adopted. Some studies have used copper, niobium, and nickel as the interlayer to prevent the formation of the compounds. Saboktakin et al. (Ref 17) used a copper interlayer in the hot roll bonding of titanium and steel. The peel strength of the bonded joints decreases with increasing bonding temperature because Ti-Cu intermetallic compounds formed at the interface. Yan et al. (Ref 18) used a nickel interlayer in the hot roll bonding of a titanium alloy and stainless steel. A maximum tensile strength of 440 MPa was obtained at a bonding temperature of 760 °C and at a reduction ratio of 20%. Ti$_2$Ni and TiNi$_3$ appeared on the fracture surface. Luo et al. (Ref 19) used a niobium interlayer in the hot roll bonding of titanium and stainless steel. A maximum interface shear strength of ∼ 396 MPa was obtained at a bonding temperature of 900 °C and at a reduction ratio of 83%. A majority of the shear fracture occurred at the Ti-Nb interface with both ductile and brittle fracture characteristics. These studies show that using an interlayer can effectively avoid the formation of compounds between titanium and steel; however, new compounds formed at the interface between the interlayer and titanium or steel at high temperature, and the compounds affected the bonding strength.

The above studies show that the temperature significantly influences the formation of the compounds. Additionally, a large deformation can be obtained by the roll bonding method, and the deformation directly influences the bonding strength. During the process of industrial production of titanium clad steel plates, adding an interlayer material will inevitably lead to an increase in production cost and an increase in the production process. Therefore, in this paper, no interlayer material was

Chao Yu, Zi-chen Qi, Hui Yu, Cheng Xu, and Hong Xiao, National Engineering Research Center for Equipment and Technology of Cold Strip Rolling, Yanshan University, Qinhuangdao 066004, Hebei, People's Republic of China; and College of Mechanical Engineering, Yanshan University, Qinhuangdao 066004, Hebei, People's Republic of China. Contact e-mail: xhh@ysu.edu.cn.

added, and the effect of bonding temperature and reduction ratio on the microstructural and mechanical properties of a hot roll bonded titanium alloy/low carbon steel plate was studied.

2. Experimental

The chemical compositions of the titanium alloy (Ti-6Al-4V) and the low carbon steel are presented in Tables 1 and 2, respectively. The thicknesses of the Ti-6Al-4V and the low carbon steel were 3 and 6 mm, respectively. The assembly pattern is shown in Fig. 1. Before assembling the billet, the oxides on the surfaces of the metals were removed using a grinding machine; then, the surfaces were repeatedly cleaned with acetone and alcohol and immediately dried. While the exterior of the assembled billet was welded, argon gas was blown into the billet through a pipe to prevent internal oxidation at the high temperature caused by the welding. Next, the pressure inside the billet was brought to 0.1 Pa via a pipe using a vacuum pump, at which point, the pipe was sealed. The size of the assembled billet was 100 mm × 50 mm × 15 mm. The rolling parameters are shown in Table 3. The billets were heated for 2 h, the rolling speed was 50 mm/s, and the billets were cooled to room temperature in the air. To exclude the influence of air entry and other accidental factors on the experimental results, three billets were rolled at each temperature, and the experiments were repeated to ensure that at least two experimental datasets were reliable.

The samples for the tension-shear test were prepared according to the specifications set in GB/T 8547-2006 (titanium clad steel plate) and GB/T 6396-2008 (clad steel plates—mechanical and technological test). Four samples of each plate were cut along the rolling direction and were tested to obtain an average shear strength. A tension-shear test was conducted using an Inspekt Table 100-kN instrument. The stretching speed was 1 mm/min. The tension-shear test sample is shown in Fig. 2. Specimens for microstructure examination were extracted along the rolling direction. The surfaces of the specimens were ground with emery papers up to No. 4000 and polished with a SiO_2 suspension with a particle size of 0.04 μm; then, the specimens were etched with a 4% nitric acid alcohol solution. The microstructure near the interface and the morphology of the fracture surface were investigated using scanning electron microscopy (SEM, Zeiss Sigma 500). The distribution of elements across the interface was examined by SEM equipped with an energy dispersive spectrometer (EDS). The interfacial compounds were analyzed using an x-ray diffractometer (XRD, D-Max 2500).

3. Results and Discussion

3.1 Interfacial Structure of the Clad Plates

Figure 3, 4, and 5 show the microstructures of the bonding interface and the shear fracture surface at bonding temperatures of 850, 950, and 1050 °C with a single-pass reduction ratio of 18%. Upon comparison with Fig. 3(a), 4(a), and 5(a), the pearlite near the interface disappeared. The recrystallization and growth of the grains in the carbon steel were obvious at 950 and 1050 °C compared with the grains at 850 °C. At 950 and 1050 °C, the grains far from the interface were pearlite and ferrite, and the grains near the interface were columnar ferrite. This suggests that the C on the steel side spread to the interface and that the reduction of C on the steel side caused pearlite to transform into ferrite. Because the EDS cannot perform quantitative analysis of ultralight elemental C, quantitative analysis of elemental C was not performed. Figure 3(b) reveals brittle fracture characteristics on the fracture surface on the Ti-6Al-4V side, indicating that brittle intermetallic compounds formed there at a bonding temperature of 850 °C. The element point scanning analysis shows that the chemical composition of the surface is similar to that of Ti-6Al-4V. The XRD analysis result indicates that C diffused from the steel to the Ti-6Al-4V side and formed the brittle compound TiC at the surface as shown in Fig. 6(a). On the fracture surface shown in Fig. 3(c) of the low carbon steel side, the elements of the surface are almost Fe. At point 2 and point 3, it is a torn feature of the carbon steel surface. This indicates that the fracture occurred mainly on the interface such as the position of point 1 in Fig. 3(c). The carbon steel and the Ti-6Al-4V bonded well only at some positions such as point 3.

Figure 4(a) shows that at 950 °C, a part of the fracture surface on the Ti-6Al-4V side has ductile fracture character-

Table 1 Chemical composition and mechanical properties of Ti-6Al-4V

Chemical composition, wt.%								Mechanical properties		
C	O	N	H	Al	V	Fe	Ti	$\sigma_{0.2}$, MPa	σ_b, MPa	δ, %
0.10	0.15	0.03	0.01	6.2	3.9	0.18	Bal.	832	910	12

Table 2 Chemical composition and mechanical properties of the steel

Chemical composition, wt.%							Mechanical properties		
C	Si	Mn	P	S	Ti	Fe	σ_s, MPa	σ_b, MPa	δ, %
0.15	0.19	0.384	0.017	0.009	0.01	Bal.	260	445	31

istics with some dimples, and the other part has brittle fracture characteristics. The element point scanning analysis shows that the content of Fe is 100% at the ductile fracture surface. Additionally, approximately 10.23% Fe dissolved in the Ti-6Al-4V matrix at the brittle fracture surface. β-Ti at the fracture surface was detected via XRD analysis, as shown in Fig. 6(b). Because Fe is a stable element of β-Ti, at high temperature, Fe dissolved in the β-Ti to form a solid solution, and when it was restored to room temperature, the solid solution no longer changed; thus, the β-Ti layer formed. Additionally, the existence of TiC indicates that the brittle compound, TiC, was mixed in the β-Ti layer. On the low carbon steel side, the fracture surface corresponds to the fracture surface of the titanium alloy side as shown in Fig. 4(c). The fractures
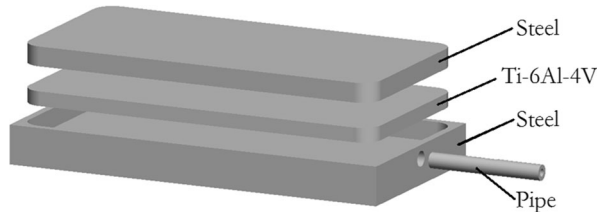
occurred partly on the low carbon steel matrix, though some occur in the brittle region with some Ti-6Al-4V matrix being torn down.

At 1050 °C, the fracture surface on the Ti-6Al-4V side showed in Fig. 5(b) is similar to the brittle fracture surface at 950 °C: There are flat surface and crack zone. However, the results of point scanning show that the content of Fe at the flat surface is ∼ 35.08% at 1050 °C; the content is much higher than that at 950 °C. From the XRD analysis of the fracture surface as shown in Fig. 6(c), at 1050 °C, TiC, Fe_2Ti, and FeTi formed at the bonding interface. At 1050 °C, a compound layer with a width of ∼ 2 µm formed at the interface. The distribution profiles of the elements across the interface between Ti-6Al-4V and steel showed that C and Fe were concentrated in the compound layer. On the low carbon steel side, there are some intermetallics on the fracture surface as at point 1 and point 2 as shown in Fig. 5(c). And some blocks of Ti-6Al-4V matrix are torn down and attached to the low carbon steel side such as the point 3 and point 4. The above results show that at 850 °C, TiC formed at the bonding interface, at 950 °C, the β-Ti layer formed at the bonding interface with TiC mixed in it, and at 1050 °C, all compounds, TiC, Fe_2Ti, and FeTi, formed at the bonding interface.

Figure 7, 8, and 9 show the microstructure of the bonding interface and the elemental distribution profiles across the interface at a bonding temperature of 850, 950, and 1050 °C

Fig. 1 Assembly pattern

Table 3 Rolling parameters and thickness ratio after rolling

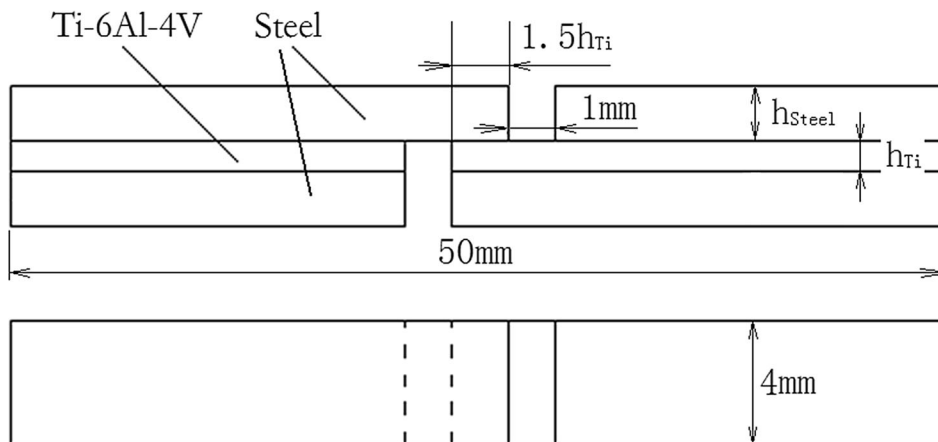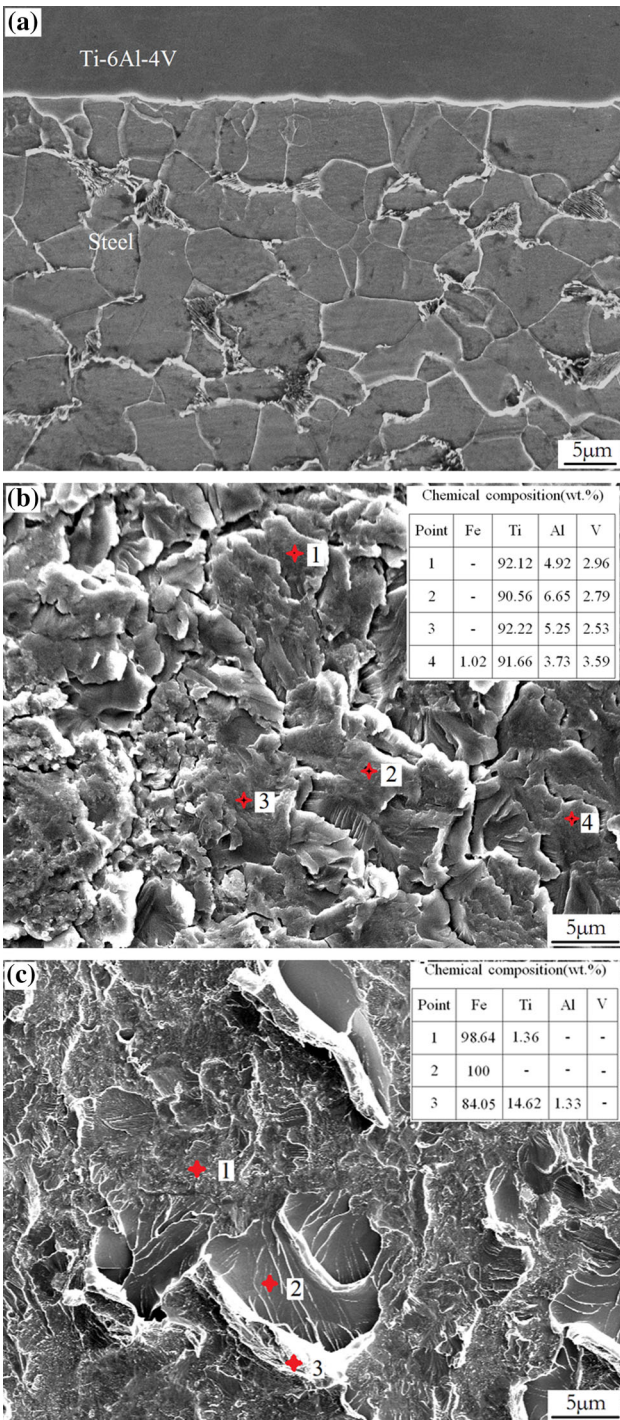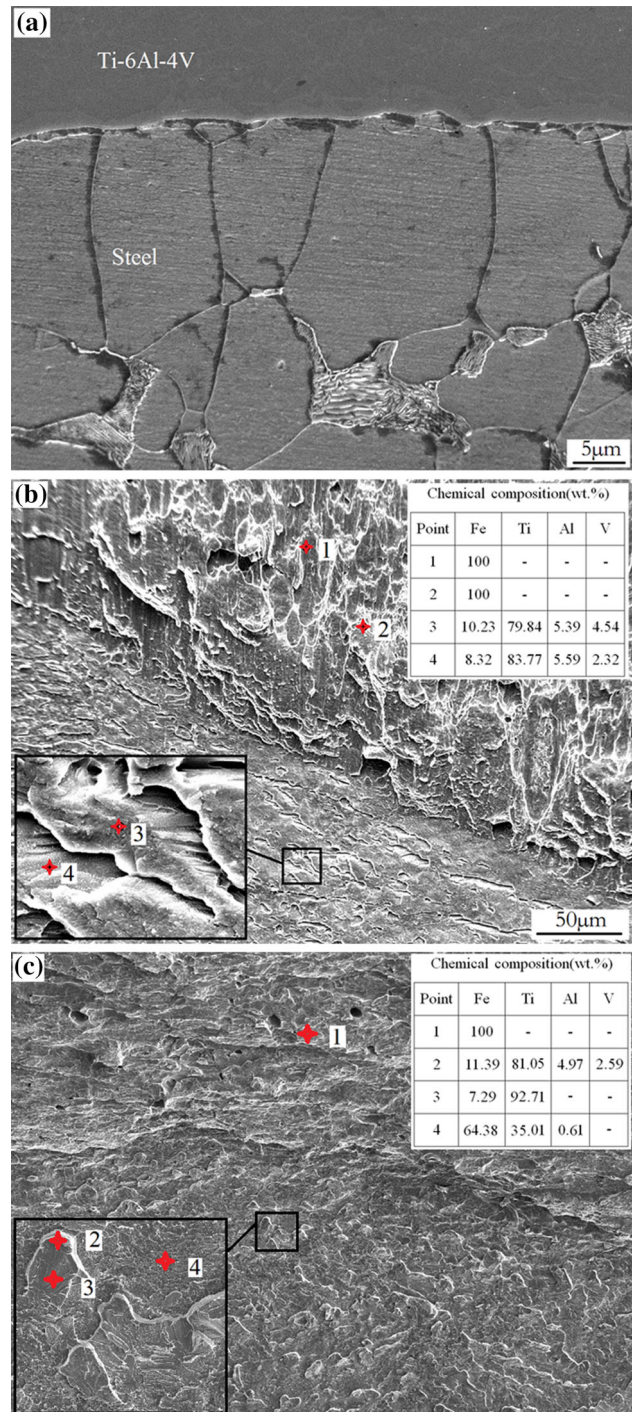| Heating temperature, °C	Total rolling pass	Total reduction ratio, %	Post-rolling temperature, °C	Thickness ratio of titanium alloy/carbon steel
850	1	18	815	0.545
	1	36	825	0.538
	2	58	726	0.542
	3	70	610	0.544
950	1	18	866	0.466
	1	36	879	0.472
	2	58	782	0.476
	3	70	691	0.481
1050	1	18	959	0.437
	1	36	971	0.443
	2	58	853	0.451
	3	70	754	0.461

Fig. 2 Schematic of the tension-shear sample

Fig. 3 SEM images of the bonding interface and the shear fracture surface at 850 °C and a 18% reduction ratio: (a) bonding interface, (b) on the Ti-6Al-4V side, (c) on the low carbon steel side

Chemical composition(wt.%) — Fig. 3(b)

Point	Fe	Ti	Al	V
1	-	92.12	4.92	2.96
2	-	90.56	6.65	2.79
3	-	92.22	5.25	2.53
4	1.02	91.66	3.73	3.59

Chemical composition(wt.%) — Fig. 3(c)

Point	Fe	Ti	Al	V
1	98.64	1.36	-	-
2	100	-	-	-
3	84.05	14.62	1.33	-

Fig. 4 SEM images of the bonding interface and the shear fracture surface at 950 °C and a 18% reduction ratio: (a) bonding interface, (b) on the Ti-6Al-4V side, (c) on the low carbon steel side

Chemical composition(wt.%) — Fig. 4(b)

Point	Fe	Ti	Al	V
1	100	-	-	-
2	100	-	-	-
3	10.23	79.84	5.39	4.54
4	8.32	83.77	5.59	2.32

Chemical composition(wt.%) — Fig. 4(c)

Point	Fe	Ti	Al	V
1	100	-	-	-
2	11.39	81.05	4.97	2.59
3	7.29	92.71	-	-
4	64.38	35.01	0.61	-

with a reduction ratio of 70%. As shown in Fig. 7(a), at 850 °C, no obvious thickness in the compound layer was found on the bonding interfaces; however, C was concentrated near the interface as shown in Fig. 7(b). This result indicates that a small amount of TiC wa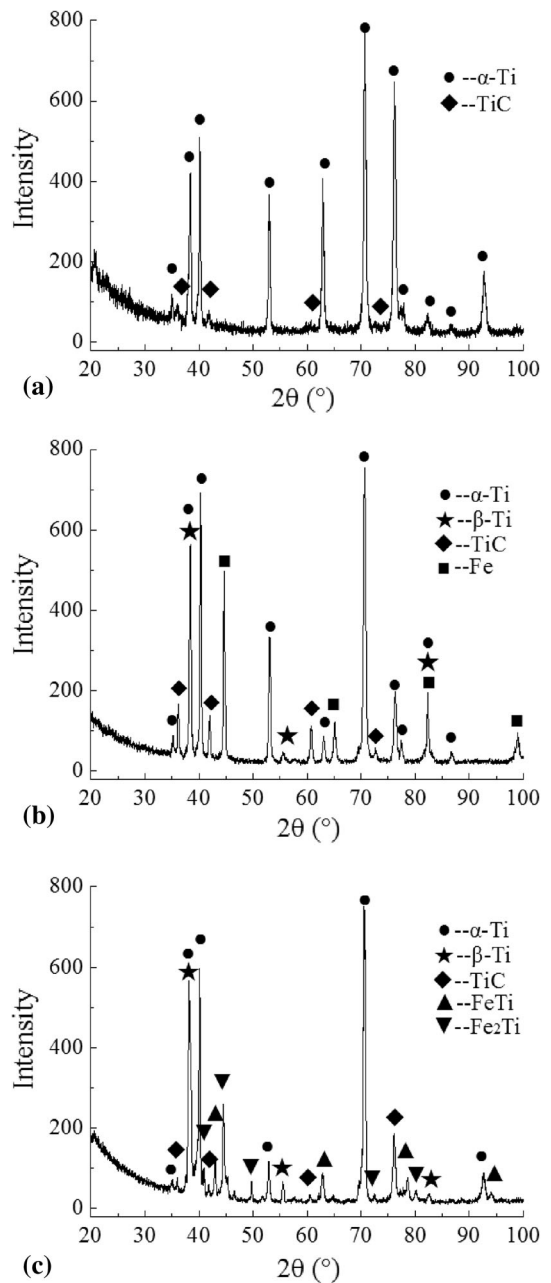s generated at the interface. As shown in Fig. 8(a), at 950 °C, a light layer of approximately 1.5 μm appears on the Ti-6Al-4V side. The element point scanning analysis shows that the content of Fe is ∼ 10.36%. From the results of the element point scanning analysis shown in Fig. 8(b), there is a step in the distribution of Fe on the light
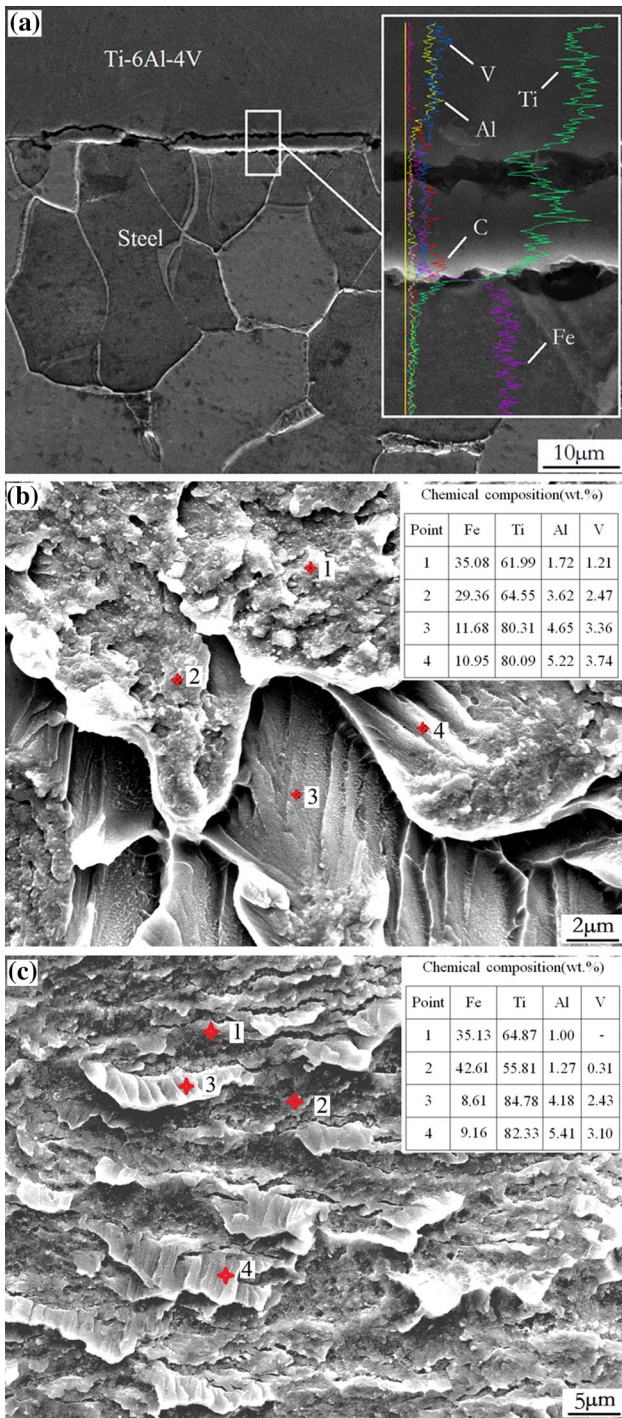
Fig. 5 SEM images of the bonding interface and the shear fracture surface at 1050 °C and a 18% reduction ratio: (a) bonding interface, (b) on the Ti-6Al-4V side, (c) on the low carbon steel side
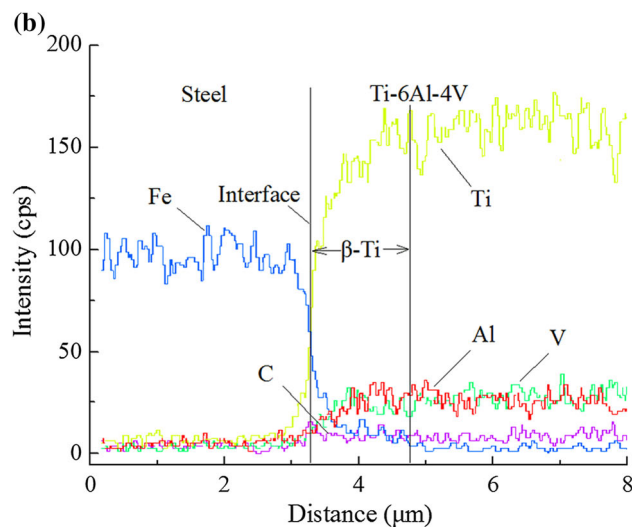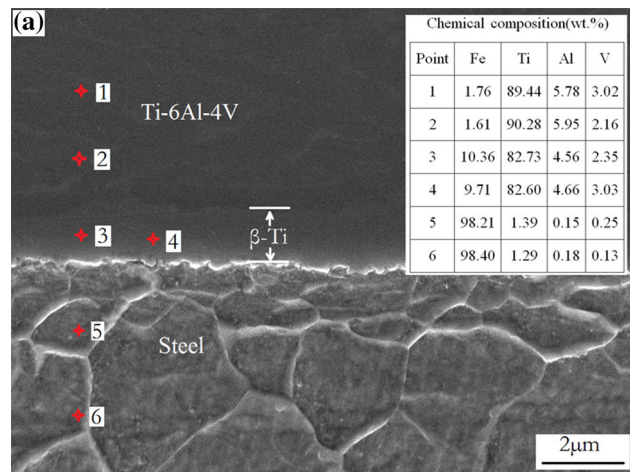

Fig. 6 XRD analysis results of the shear fracture surface on the Ti-6Al-4V side at an 18% reduction ratio: (a) 850 °C, (b) 950 °C, (c) 1050 °C

layer, which indicates that the light layer is the β-Ti layer. The increased distribution of C on the Ti-6Al-4V matrix indicates that TiC is distributed in the Ti-6Al-4V matrix near the interface. The element diffusion distance between the Ti-6Al-4V and steel is approximately 2 μm.

At 1050 °C, the bonding interfaces at reduction ratio of 36, 58, and 70% are shown in Fig. 9. At high heating temperature, compound layer formed at the interface as shown in Fig. 5(a) and (b). In the multi-pass rolling process, the compound layer was broken during deformation, and the compounds were discontinuously distributed at the interface to form the dark layer. Meanwhile, the fresh metal of the Ti-6Al-4V matrix and the steel matrix was squeezed out and bonded at a high rolling force and high temperature. Finally, a new bonding zone

Fig. 7 At 850 °C and at a 70% reduction ratio: (a) SEM of the interface, (b) EDS of the interface
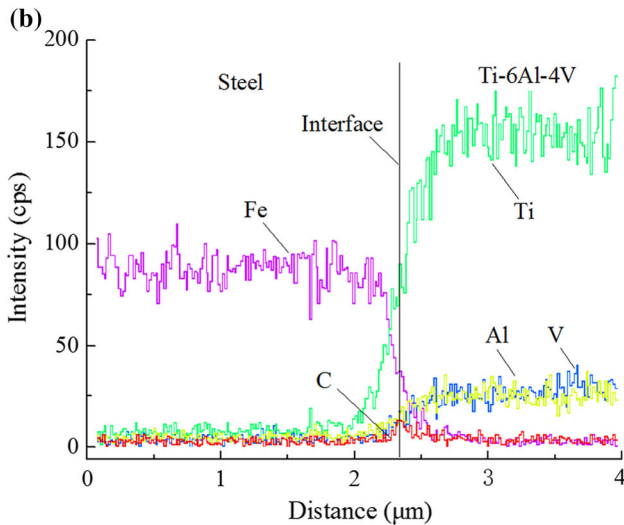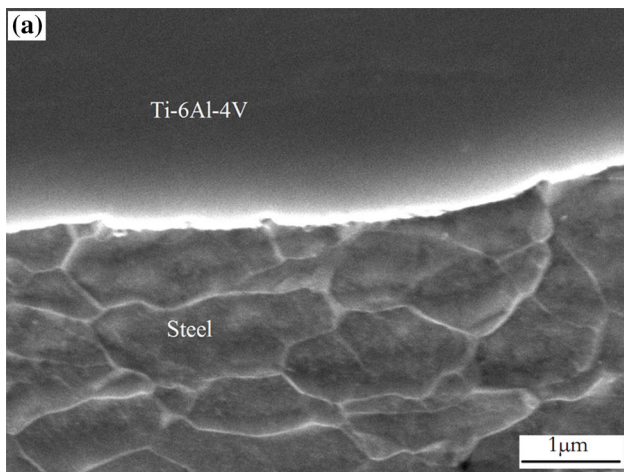
Fig. 8 At 950 °C and at a 70% reduction ratio: (a) SEM of the interface, (b) EDS of the interface

formed as the light layer as shown in Fig. 9(a), (b), and (c). Comparing the line scanning analysis results of the light layer between Fig. 8(b) and 9(e), the elemental distributions are similar and the light layer is β-Ti. As shown in Fig. 9(c), the line scanning analysis result of the dark layer is similar to the scanning result of the compound layer in Fig. 3(e) and the elemental distribution profiles across the interface show that C concentrated in the dark layer. For Ti is a strong combining element of C and TiC is easily formed, and the XRD result showed in Fig. 6(c) indicates TiC formed on the interface, the dark layer was mixed with TiC. At 1050 °C, the Ti and Fe diffusion distance between Ti-6Al-4V and steel is ~ 1 μm in the light layer, and in the dark layer, the distance is ~ 1.5 μm. They are all shallower than the diffusion distance at 950 °C. This indicates that the compound generation hindered the diffusion between Ti and Fe.

Figure 10, 11, and 12 show the microstructure of the bonding interface at a bonding temperature of 850, 950, and 1050 °C with a reduction ratio of 70%. At 850 °C, a small number of dimples are distributed on the shear fracture surface, and there are simultaneous brittle fracture characteristics as shown in Fig. 10(b). From the point scanning analysis shown in Fig. 10(c), the content of Fe in the dimples zone was close to 100%, and the chemical composition in the brittle fracture zone was close to that of the Ti-6Al-4V matrix. This result indicates that part of the fracture occurred on the steel matrix and that part of it occurred on the side of the Ti-6Al-4V matrix mixed with some compounds there. When the bonding temperature was 950 °C and the rolling reduction ratio was 70%, a large number of dimples were distributed on the fracture surface, as shown in Fig. 11. The results of the point scanning analysis show that the content of Fe at the fracture surface was 100%,
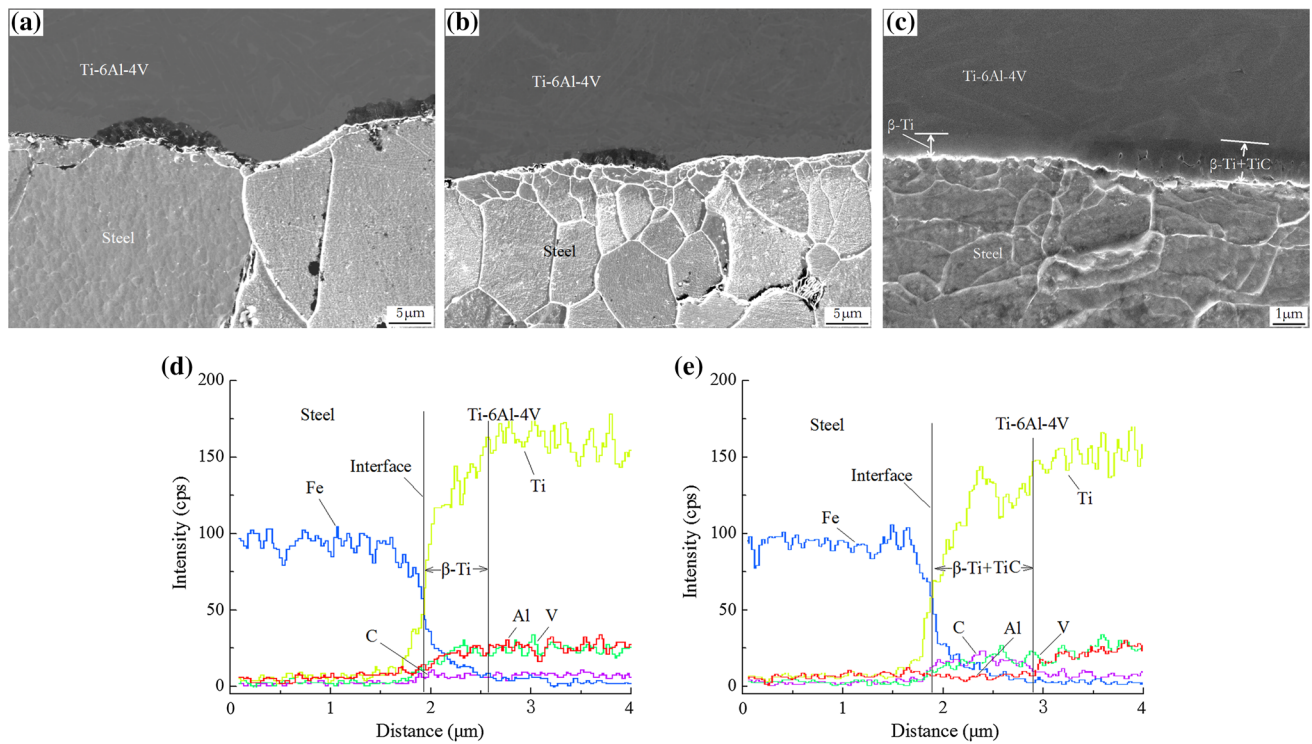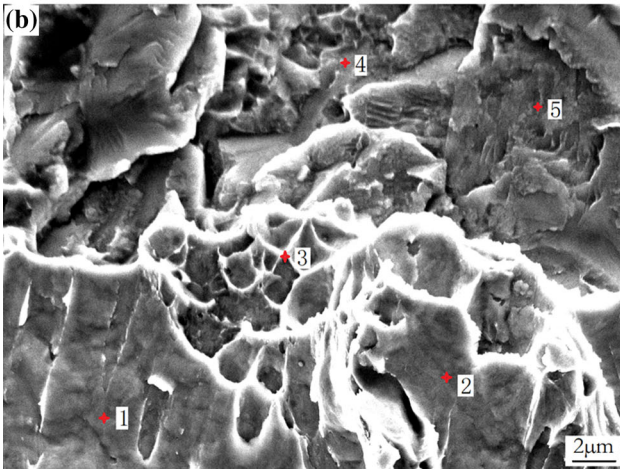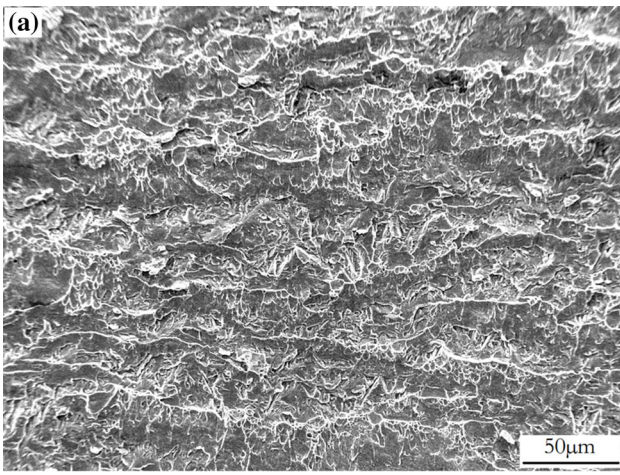
Fig. 9 At 1050 °C, SEM of the interface: (a-c) at 36, 58, 70% reduction ratio, (d) EDS of the light layer, (e) EDS of the dark layer

indicating that the shear fracture occurred on the steel matrix side. At 1050 °C and at a 70% reduction ratio, a shear fracture surface was observed as shown in Fig. 12. The content of Fe was close to 100% at points 1 and 2, and dimples appeared there. Thus, it was a steel matrix at the position of points 1 and 2. At point 3, the Fe and Ti contents were 52.14 and 44.61%, and Fe-Ti compounds possibly were present. At points 4 and 5, the Fe contents were 18.65 and 13.47%. There may be a β-Ti layer mixed with some Fe-Ti compounds. The layered fracture structure shows that at 1050 °C, the compound layer was broken during the multi-pass rolling process, and a good combination between the extruded fresh metal of the Ti-6Al-4V matrix and the steel matrix was again achieved. However, due to the high temperature, more compounds were generated, and the compounds were crack sources, and in the shear force, the fracture started from the crack sources, leading subsequently to the surrounding good bonded part began to fracture.

3.2 Macroscopic Bonding Property Test of the Clad Plates

Figure 13 shows plots of the variations in the shear strength with bonding temperature and total reduction ratio. When the reduction ratio is between 18 and 70%, the shear strength increases with an increasing reduction ratio. During the heating process, some compounds formed on the interface and affect the bonding strength. With the increase in reduction ratio, the

compound layer on the interface was broken more fully as shown in Fig. 9(a), (b), and (c). During the multi-pass rolling process, the matrix metals on both sides were extruded and formed new bonding region. Otherwise, work hardening existed in multi-pass rolling process for the reduction in rolling temperature. Under the influence of these comprehensive factors, the shear strength increases with the increasing reduction ratio. At 950 °C, when the reduction ratio is larger than 36%; at 850 °C, when the reduction ratio is larger than 58%; and at 1050 °C, when the reduction ratio is 70%, the interfacial shear strength of the composite plate reaches the standard value of 196 MPa from the GB/T 8547-2006 type 0 titanium clad steel plate. At 850 and 1050 °C, when the reduction ratio is less than 36%, the shear strength of the composite plate cannot reach the standard value of 140 MPa from the GB/T 8547-2006 type 1 titanium clad steel plate. At 950 °C and at a 70% reduction ratio, the shear strength of the interface reaches a maximum of 329.5 MPa and the fracture occurs on the steel matrix, indicating that under this condition, the interface bonded well and the strength of the bonding layer on the interface is higher than that of the steel matrix. At 950 °C, at each reduction ratio, the shear strength is higher than that at 850 and 1050 °C. This is because at 850 °C, the bonding temperature is low, and element diffusion between the titanium alloy and steel is not sufficient, which lowers the bonding
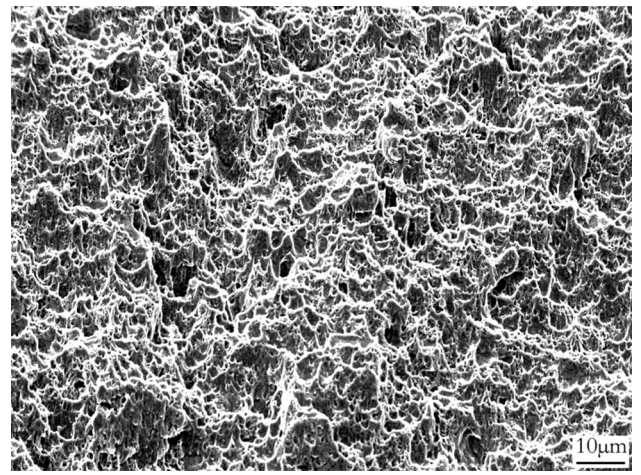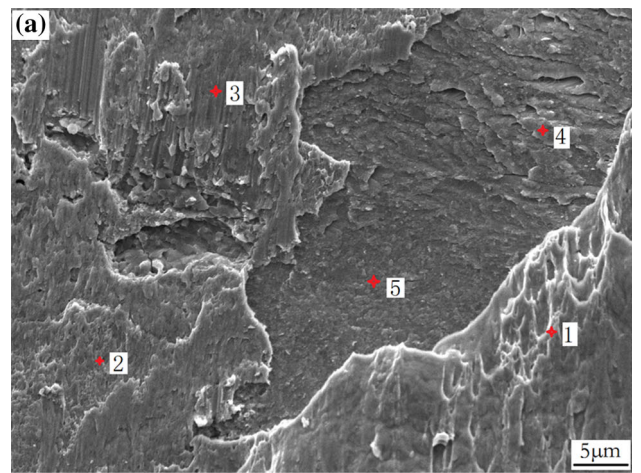
Fig. 11 SEM images of the shear fracture surface at 950 °C and at a 70% reduction ratio

(a)

(b) Chemical composition(wt.%)

Point	Fe	Ti	Al	V
1	99.52	0.48	0	0
2	99.16	0.84	0	0
3	52.14	44.61	1.61	1.64
4	18.65	75.93	2.96	2.46
5	13.47	79.26	4.23	3.04

Fig. 12 SEM images of the shear fracture surface at 1050 °C and at a 70% reduction ratio: (a) microstructure, (b) results of point scanning

(c) Chemical composition(wt.%)

Point	Fe	Ti	Al	V
1	96.65	3.35	0	0
2	98.12	1.88	0	0
3	96.34	3.66	0	0
4	1.72	88.60	6.49	3.19
5	0	89.66	7.21	3.13

Fig. 10 SEM images of the shear fracture surface at 850 °C and at a 70% reduction ratio: (a) overall morphology, (b) microstructure, (c) results of point scanning

strength. At 1050 °C, the bonding strength decreased because more compounds formed on the interface. When the reduction ratio was less than 36%, the shear strength at 850 °C was lower than that at 1050 °C. When the reduction ratio was greater than 58%, the shear strength at 850 °C was higher than that at 1050 °C. This is probably because, at a small reduction ratio

and at a low temperature of 850 °C, the contact surfaces of Ti-6Al-4V and steel are not easy to deform, the contact surfaces are not tight enough, and the diffusion is not sufficient, resulting in a lower bond strength. However, at a large
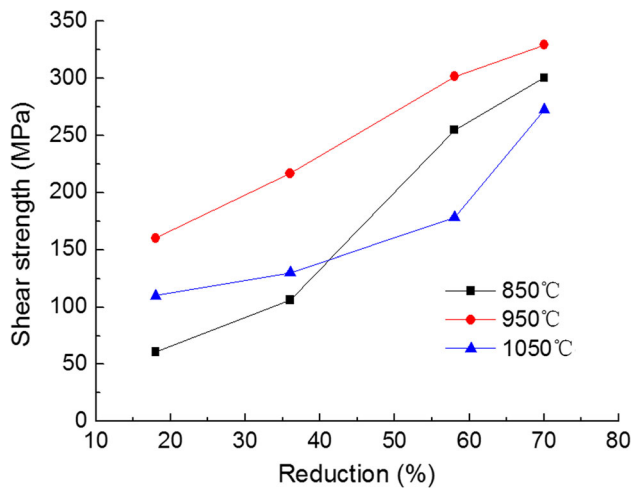
Fig. 13 Variations in the shear strength as a function of bonding temperature and total reduction ratio

reduction ratio and at 1050 °C, due to the complex compounds distributed at the interface, the bonding strength was reduced.

4. Conclusions

1. A titanium alloy and low carbon steel were bonded via hot rolling in a vacuum. When the rolling speed is 50 mm/s, the bonding temperature is between 850 and 1050 °C and the shear strength of the bonding interface increases with a reduction ratio from 18 to 70%. Additionally, at 950 °C and at a reduction ratio of 70%, the bonding result is the best, and the shear fracture occurs on the steel matrix.
2. At bonding temperatures of 850 and 950 °C, TiC forms at the interface and few FeTi and Fe_2Ti form. At 1050 °C, besides the formation of TiC, many FeTi and Fe_2Ti form at the interface, which decreases the bonding strength.
3. Using the multi-pass rolling process to obtain a large reduction ratio, it is beneficial to break the compound layer and the extrusion of the fresh metal; thus, good bonding can be again achieved between the extruded fresh metals.

References

1. S.A.A.A. Mousavi and P.F. Sartangi, Experimental Investigation of Explosive Welding of cp-Titanium/AISI, 304 Stainless Steel, *Mater. Des.*, 2009, **30**(3), p 459–468
2. J.S. Ha and S.I. Hong, Deformation and Fracture of Ti/439 Stainless Steel Clad Composite at Intermediate Temperatures, *Mater. Sci. Eng. A*, 2016, **651**, p 805–809
3. T.N. Prasanthi, R.C. Sudha, and S. Saroja, Explosive Cladding and Post-Weld Heat Treatment of Mild Steel and Titanium, *Mater. Des.*, 2016, **93**, p 180–193
4. J. Song, A. Kostka, M. Veehmayer, and D. Raabe, Hierarchical Microstructure of Explosive Joints: Example of Titanium to Steel Cladding, *Mater. Sci. Eng. A*, 2011, **528**(6), p 2641–2647
5. H. Su, X.B. Luo, F. Chai, J.C. Shen, X.J. Sun, and F. Lu, Manufacturing Technology and Application Trends of Titanium Clad Steel Plates, *J. Iron Steel Res. Int.*, 2015, **22**(11), p 977–982
6. N. Kahraman, B. Gülenç, and F. Findik, Joining of Titanium/Stainless Steel by Explosive Welding and Effect on Interface, *J Mater. Process. Technol.*, 2005, **169**(2), p 127–133
7. P. Manikandan, K. Hokamoto, M. Fujita, K. Raghukandan, and R. Tomoshige, Control of Energetic Conditions by Employing Interlayer of Different Thickness for Explosive Welding of Titanium/304 Stainless Steel, *J Mater. Process. Technol.*, 2008, **195**(1–3), p 232–240
8. C. Velmurugan, V. Senthilkumar, S. Sarala, and J. Arivarasan, Low Temperature Diffusion Bonding of Ti-6Al-4V and Duplex Stainless Steel, *J Mater. Process. Technol.*, 2016, **234**, p 272–279
9. M. Wachowski, M. Gloc, T. Ślęzak, T. Płociński, and K.J. Kurzydłowski, The Effect of Heat Treatment on the Microstructure and Properties of Explosively Welded Titanium-Steel Plates, *J. Mater. Eng. Perform.*, 2017, **26**(3), p 945–954
10. M.X. Xie, L.J. Zhang, G.F. Zhang, J.X. Zhang, Z.Y. Bi, and P.C. Li, Microstructure and Mechanical Properties of CP-Ti/X65 Bimetallic Sheets Fabricated by Explosive Welding and Hot Rolling, *Mater. Des.*, 2015, **87**, p 181–197
11. D.S. Zhao, J.C. Yan, Y. Wang, and S.Q. Yang, Relative Slipping of Interface of Titanium Alloy to Stainless Steel During Vacuum Hot Roll Bonding, *Mater. Sci. Eng. A*, 2009, **499**(1–2), p 282–286
12. T. Momono, T. Enjo, and K. Ikeuchi, Effect of Carbon Content on the Diffusion Bonding of Iron and Steel to Titanium, *ISIJ Int.*, 1990, **30**(11), p 978–984
13. C. Yu, H. Xiao, H. Yu, Z.C. Qi, and C. Xu, Mechanical Properties and Interfacial Structure of Hot-Roll Bonding TA2/Q235B Plate Using DT4 Interlayer, *Mater. Sci. Eng. A*, 2017, **695**, p 120–125
14. H.T. Jiang, X.Q. Yan, J.X. Liu, and X.G. Duan, Effect of Heat Treatment on Microstructure and Mechanical Property of Ti—Steel Explosive-Rolling Clad Plate, *Trans Nonferr. Met. Soc.*, 2014, **24**(3), p 697–704
15. I.K. Kim and S.I. Hong, Effect of Heat Treatment on the Bending Behavior of Tri-Layered Cu/Al/Cu Composite Plates, *Mater. Des.*, 2013, **47**(9), p 590–598
16. I.K. Kim and S.I. Hong, Effect of Component Layer Thickness on the Bending Behaviors of Roll-Bonded Tri-Layered Mg/Al/STS Clad Composites, *Mater. Des.*, 2013, **49**, p 935–944
17. M. Saboktakin, G.R. Razavi, and H. Monajati, The Investigate Metallurgical Properties of Roll Bonding Titanium Clad Steel, *Int. J Appl. Phys. Math.*, 2011, **1**, p 177–180
18. J.C. Yan, D.S. Zhao, C.W. Wang, and S.Q. Yang, Vacuum Hot Roll Bonding of Titanium Alloy and Stainless Steel Using Nickel Interlayer, *Mater. Sci. Technol. Lond*, 2013, **25**(7), p 914–918
19. Z.A. Luo, G.L. Wang, G.M. Xie, L.P. Wang, and K. Zhao, Interfacial Microstructure and Properties of a Vacuum Hot Roll-Bonded Titanium-Stainless Steel Clad Plate with a Niobium Interlayer, *Acta Metal. Sin.*, 2013, **26**(6), p 754–760